J Solid State Electrochem (2010) 14:2107–2112
DOI 10.1007/s10008-010-1052-6

ORIGINAL PAPER

High-performance Fe–Co-based SOFC cathodes

Kent Kammer Hansen · Karin Vels Hansen · Mogens Mogensen

Received: 24 October 2009 / Accepted: 12 March 2010 / Published online: 30 March 2010

Abstract With the aim of reducing the temperature of the solid oxide fuel cell (SOFC), a new high-performance perovskite cathode has been developed. An area-specific resistance (ASR) as low as 0.12 Ωcm^2 at 600 °C was measured by electrochemical impedance spectroscopy (EIS) on symmetrical cells. The cathode is a composite between $(Gd_{0.6}Sr_{0.4})_{0.99}Fe_{0.8}Co_{0.2}O_{3-\delta}$ (GSFC) and $Ce_{0.9}Gd_{0.1}O_{1.95}$ (CGO10). Examination of the microstructure of the cathodes by scanning electron microscopy (SEM) revealed a possibility of further optimisation of the microstructure in order to increase the performance of the cathodes. It also seems that an adjustment of the sintering temperature will make a lowering of the ASR value possible. The cathodes were compatible with ceria-based electrolytes but reacted to some extent with zirconia-based electrolytes depending on the sintering temperature.

Introduction

The SOFC is an all-solid-state device that can convert chemical energy directly into heat and electricity [1]. The SOFC is normally constructed from a Ni-YSZ (YSZ = yttria-stabilised zirconia) composite anode, a YSZ-electrolyte and a LSM/YSZ (LSM = strontium-substituted lanthanum manganite) composite cathode. In order to lower the operation temperature of the fuel cell new anode, electrolyte and cathode materials are needed. In this text, emphasis is put on cathodes. Many attempts have been done to replace the conventional LSM/YSZ composite cathode with cathodes with a higher performance, see, e.g. [2]. The general problem is that the alternative cathode materials react with the zirconia-based electrolytes, and form insulating layers at the interface between the electrolyte and the cathode [3]. This problem can be overcome by adding a barrier layer of doped ceria between the zirconia-based electrolyte and the cathode [4]. This is not without problems but it seems to be the most feasible pathway. Addition of a barrier layer makes cobalt-containing cathodes a possible choice. It is known that cobalt-containing perovskite cathodes have a performance superior to the LSM/YSZ composite cathode [5]. However, an additional problem in the use of cobalt-containing cathodes is that the thermal expansion coefficient (TEC) of the cobalt-containing cathodes is very high [6]. This might make thermal cycling of the cathodes impossible. To some extent, this problem can be solved or at least minimised if the cathodes are made as composites with the electrolyte powder.

The cobalt-containing cathodes studied the most in literature seems to be composites of $Sm_{0.5}Sr_{0.5}CoO_{3-\delta}$ or $La_{0.6}Sr_{0.4}Fe_{0.8}Co_{0.2}O_{3-\delta}$ with a ceria-based electrolyte powder [7–10]. An example of the performance of a $Sm_{0.5}Sr_{0.5}CoO_{3-\delta}$ composite cathode can be found in [7]. The ASR value measured at 600 °C was 0.18 Ωcm^2. However, the TEC of $Sm_{0.5}Sr_{0.5}CoO_{3-\delta}$ is very high as it is a pure cobaltite perovskite, which may make the practical application of this material difficult. The lowest value measured on the $La_{0.6}Sr_{0.4}Fe_{0.8}Co_{0.2}O_{3-\delta}$ perovskite is 0.33 Ωcm^2 at 600 °C [10]. Others have tried to improve the performance of the $La_{0.6}Sr_{0.4}Fe_{0.8}Co_{0.2}O_{3-\delta}$-based cathodes, especially at low temperature, by adding Pd [8]. However, no value below 0.33 Ωcm^2 at 600 °C was obtained. Wei et al. [11] showed that an A-site-deficient

K. K. Hansen (✉) · K. V. Hansen · M. Mogensen
Fuel Cells and Solid State Chemistry Division,
Risø National Laboratory for Sustainable Energy,
Technical University of Denmark,
4000 Roskilde, Denmark
e-mail: kkha@risoe.dtu.dk

Table 1 Experimental matrix for the development of high-performance cathodes

Temperature	850°C	900°C	950°C	1000°C	1050°C
70/30% (*w*/*w*)	S1	S2	S3	S6	S7
60/40% (*w*/*w*)	–	–	S4	–	–
50/50% (*w*/*w*)	–	–	S5	–	–

$(La_{0.6}Sr_{0.4})_sFe_{0.8}Co_{0.2}O_{3-\delta}$ perovskite cathode had a higher performance than the stoichiometric perovskite. Recently, even lower ASR values were obtained with a $Ba_{0.5}Sr_{0.5}Fe_{0.2}Co_{0.8}O_{3-\delta}$-based cathode [12]. An ASR value less than 0.1 Ωcm^2 were found at 600 °C. This study describes the initial development of a GSFC/CGO10 composite cathode. The cathode material and the composite cathodes were characterised by powder X-ray diffraction (XRD), particle-size distribution (PSD), SEM and by EIS on symmetrical cells of the type GSFC+CGO10/CGO10/GSFC+CGO10. Some studies of Gd containing Fe–Co-based cathodes have already been undertaken and it was shown that they have a performance superior to La-containing Fe–Co-based cathodes [13].

Experimental

The CGO10 powder was used as received from Rhodia. According to the supplier, the surface area of the powder was around 20–25 m^2/g. Synthesis of GSFC was performed using the glycine–nitrate method described elsewhere [14]. As starting materials, metal–nitrates with a purity in excess of 99% were used. The powder was calcined at 1,100 °C/2 h before use. This assured that a material containing only perovskite phases was obtained. The powder was characterised by powder XRD using a Stoe diffractometer with $Cu_{k\alpha}$ radiation. CGO10 was used as an electrolyte (in two cases, YSZ was used as an electrolyte in order to evaluate the stability of the cathodes towards YSZ). CGO10 plates were either supplied by InDEC BV or made in-house by conventional tape casting. The YSZ plates were made in-house likewise by conventional tape casting. The thickness of the plates was around 200 μm and the size of the plates was approximately 50×50 mm^2. The cathodes were fabricated by slurry spraying on the pre-sintered plates of ceria or zirconia-based electrolytes. The slurries for the spraying were made by mixing the powders with an appropriate binder and a solvent in a ball mill. Three different slurries were made, one with 70% perovskite and 30% CGO10 (wt.%, slurry number 1), one with 60% perovskite and 40% CGO10 (slurry number 2) and one with 50% perovskite and 50% CGO10 (slurry number 3). The slurries were characterised by measuring the PSD using a Beckman-Coultier LS 13 320 particle-size analyser. The cathodes were added in two layers with intermediate sintering. The first layer had a thickness of approximately 15 μm and the second layer a thickness of approximately 10 μm. Along with different sintering temperatures different compositions were evaluated in order to optimise the cathodes. The experimental matrix is given in Table 1. Only the cells fabricated using ceria plates are given in Table 1. Cells of cathodes made on zirconia plates were sintered at 900 or 1,000 °C. These cells are named Z900 and Z1000. Slurry number 1 was used for the fabrication of these cells. The lowest sintering temperature (850 °C) was not useful, as the electrode was not attached properly to the electrolyte and no further actions were taken with these cells. Before the microscopy investigation and the electrochemical measurements, the plates were cut into smaller pieces with a size of approximately 4×4 mm^2. For the structural investigation of the cathodes, SEM analysis was undertaken

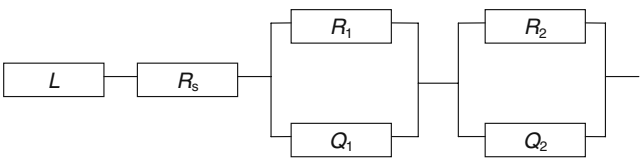

Fig. 1 Equivalent circuit used for typical fit of EIS data

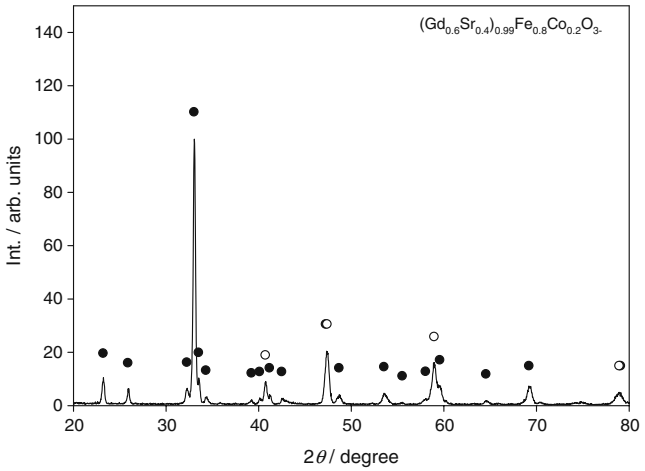

Fig. 2 XRD pattern of $(Gd_{0.6}Sr_{0.4})_{0.99}Fe_{0.8}Co_{0.2}O_{3-\delta}$. *Filled circles* are orthorhombic phase, *open circles* are cubic phase. Cubic phase is only indicated where it does not coincide with the orthorhombic phase

Table 2 Lattice parameters for the two perovskite phases (in the mixture with the nominal composition $(Gd_{0.6}Sr_{0.4})_{0.99}$ $Fe_{0.8}Co_{0.2}O_{3-\delta}$) and $GdFeO_{3-\delta}$

Unit cell axis	Cubic phase (Å)	Orthorhombic phase (Å)	$GdFeO_{3-\delta}$ (Å)
a	3.8270	7.6243	7.668
b	3.8270	5.5572	5.616
c	3.8270	5.3276	5.346

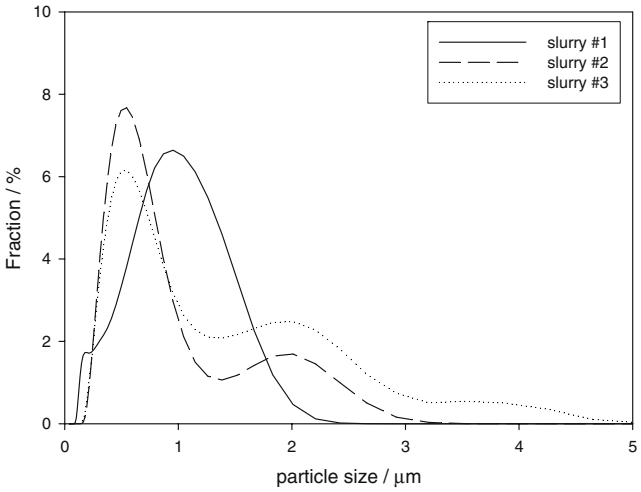

Fig. 3 Particle-size distribution of the slurries used for the fabrication of the cathodes

using a JEOL JSM-840 SEM instrument. The cells for the SEM analysis were casted in epoxy and polished to obtain SEM micrographs of the cross section of the cells.

The performance of the cathodes was evaluated by EIS using a Solartron 1260 frequency response analyser. For the measurements, an amplitude of 25–50 mV was used. The frequency range spanned was 1 MHz to 50 mHz with five points measured at each decade. An integration time of five cycles was used throughout. For the recordings of data, an in-house PC-DOS programme was used. Before the electrochemical measurements, a layer of platinum paste was added on the top of the electrodes. The platinum paste used has the code Pt#308 and it was used as received from Degussa. The platinum layer acted as a current collector as the in-plane conductivity of the cathodes was insufficient. The platinum layer was sintered in situ at 800 °C.[1] Measurements were recorded at temperatures of 800, 700 and 600 °C after steady state was obtained (2 h). The obtained data were fitted using the programme equivcrt by Boukamp [15]. In general, the data were fitted using as few *RQ* components as possible while still obtaining a good fit. *R* is a resistance and *Q* a constant phase element. A typical example of an equivalent circuit used for the fittings is given in Fig. 1. In the figure, *L* is an inductance coming from the wires. The summit frequencies of the individual arcs were calculated as [16]

$$f_{\text{summit}} = \tfrac{1}{2\pi}(\mathrm{R}Y_o)^{-1/n}, \quad (1)$$

Where *R* is the resistance of the arc, Y_0 an admittance, and *n* is the frequency exponent.

[1] The exact procedure should be followed in order to obtain the low ASR values reported in this study.

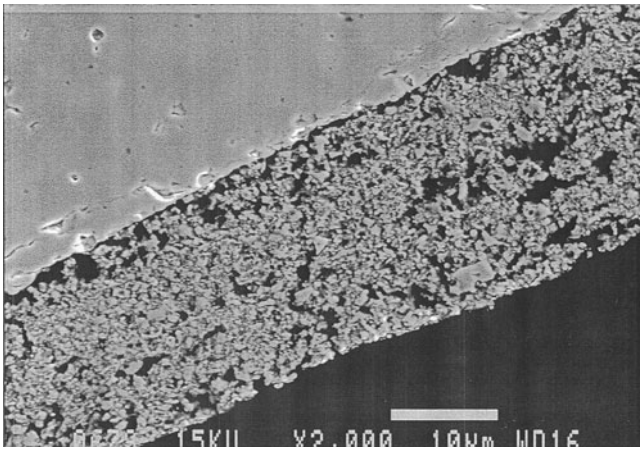

Fig. 4 SEM picture of a cathode sintered at 950 °C

Results

The XRD powder pattern of the calcined GSFC powder can be found in Fig. 2. As it can be seen, the powder was a mixture of two phases, an orthorhombic perovskite phase and a cubic perovskite phase. The unit cell parameters from the refinements can be found in Table 2 together with the values for the parent compound $GdFeO_{3-\delta}$. Lower calcination temperatures (less than 1,000 °C) resulted in a powder of mixed phases (also non-perovskite phases).

The PSD of the three cathode slurries can be found in Fig. 3. The PSD consists of contributions from the ceria and the perovskite powders. The average particle size was in the range 0.15–2 μm with a small fraction of particles with a size of approximately 4 μm for one of the slurries (slurry number 3).

The SEM micrograph of one of the investigated cells can be found in Fig. 4. In general, the porosity of the cells was low and the pores were uneven of size and distribution. The particle size evaluated on the background of the SEM micrographs was below 1 μm. The cathodes seem well-adhered to the electrolyte.

An example of the results of the electrochemical measurements on the symmetrical cells can be found in

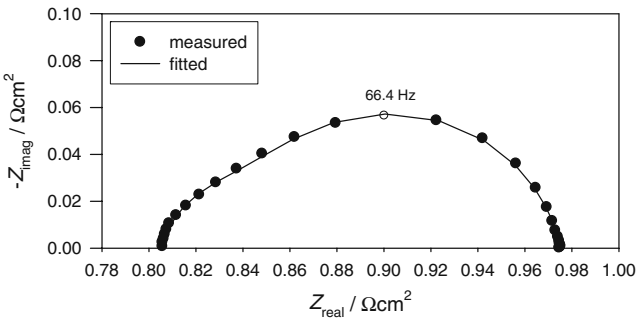

Fig. 5 EIS spectra of sample S7 recorded at 600 °C in air. Corrected for inductance in the wires

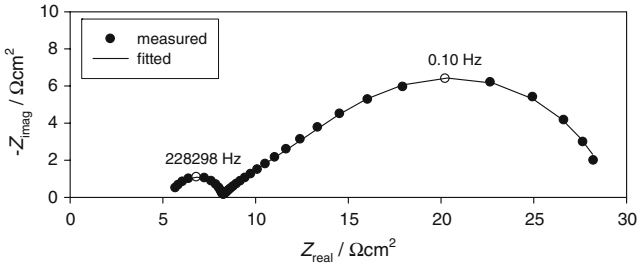

Fig. 6 EIS spectra of sample S7 recorded at 400 °C in air

Fig. 5. The spectrum shown is for sample S7 at a measured temperature of 600 °C. The spectra reveal typically from 1 to 3 depressed semi-circles depending on the sample and the temperature of the measurement. If the measurements were continued at temperatures below 600 °C, an additional arc was revealed, see Fig. 6. This arc was a high-frequency arc with a high summit frequency. The ASR values obtained from the fitting of the spectra for sample no. S7 can be found in Table 3. The summit frequencies of the different arcs can likewise be found in Table 3. The total ASR values obtained by fitting of the measurements can be found in Table 4. The ASR values obtained on YSZ are much higher than for the cells prepared on CGO10. The activation energies are listed in Table 5. An activation energy plot of the medium frequency arc for the sample 7 can be found in Fig. 7.

Discussion

The powder XRD revealed that the powder was a two phase system. This has also been shown in the literature for similar compounds [17]. The crystallinity was not very high (evaluated on the background of line width) and it is more difficult to obtain powders consisting of only perovskite phases when Gd(III) is used as an A-site cation, than for larger A-site cations like La(III) or Pr(III). This is in accordance with the literature [18]. This might be due to a larger difference in size of the A-site cations as the ionic radii of Gd(III) is smaller than the ionic radii of La(III) and Pr(III). This will give rise to tension in the lattice of the perovskite. The crystal system of the orthorhombic perovskite phase is equal to the crystal system of the parent compound $GdFeO_{3-\delta}$ [19]. The unit cell of $GdFeO_{3-\delta}$ is slightly larger than the unit cell of the cobalt-containing orthorhombic perovskite phase. This might be due to differences between the size of the iron and cobalt ions, cobalt is slightly smaller than iron [20]. In addition to this, the B-site cations are more oxidised when Sr(II) is replaced by Gd(III) leading to higher concentrations of Fe(IV) and Co(IV) with a thereof lower average size of the B-site cations.

The SEM micrographs revealed that there still is room for improvement as the structure is not porous enough. It also seems like that the adhesion to the electrolyte is insufficient when a sintering temperature below 900 °C is used. This result in cells with higher ASR values than for the electrodes sintered at higher temperatures. The microstructure of the cathodes depend only slightly on the sintering temperature, as only minor differences in the microstructure of the cathodes are revealed by the SEM micrographs. However, the sample sintered at 900 °C seems to be more porous than the other cells. The effect of sintering temperature is most likely due to a better adhesion of the cathodes to the electrolyte and a better particle–particle contact than for the cathodes fabricated using a lower sintering temperatures. The difference is not large but it is significant. Better composite cathodes might therefore be fabricated if the composite cathodes with a high CGO10 content are processed at higher temperatures than the cathodes investigated in this study. It can also be seen that the reactivity of the cathode towards zirconia is markedly decreased when the sintering temperature is lowered from 1,000 °C to 900 °C. However, the ASR values obtained from processing the cathodes at 900 °C are still too high for practical applications in the low temperature limit of the SOFC. In fact, the performance is slightly lower than for high-performance LSM/YSZ cathodes [21]. It is also likely that the values of ASR will increase as a function of time due to further reaction between the cathode and the zirconia-based electrolyte. The high ASR values obtained for the cathodes fabricated on zirconia is most likely due to the formation of $SrZrO_3$ as the compound $GdCoO_{3-\delta}$ is reported to be stable towards zirconia [4]. The replacements of strontium with calcium can possible solve or significant-

Table 3 Fitted ASR values and summit frequencies of sample S7

Parameter/temp.	600°C	700°C	800°C
R_s	0.81 Ωcm^2	0.28 Ωcm^2	0.01 Ωcm^2
R_1	0.04 Ωcm^2	0.48 Ωcm^2	0.01 Ωcm^2
$F_{summit,\ 1}$	804 Hz	723 Hz	4000 Hz
R_2	0.14 Ωcm^2	–	8×10^{-4} Ωcm^2
$F_{summit,\ 2}$	58 Hz	–	21 Hz

Table 4 ASR values for the electrodes in mΩcm^2 for the electrodes on CGO10

Temp/nr	S4	S5	S2	S3	S6	S7	Z1000	Z900
600 °C	116.7	114.1	305.3	211.1	187.6	169.8	364 Ω	12.8 Ω
700 °C	31.9	25.4	46.4	46.2	37.6	38.6	30.4 Ω	1.92 Ω
800 °C	12.6	11.0	18.3	11.6	13.2	12.4	3.5 Ω	392

Note that for the electrodes on YSZ the ASR values are in Ωcm^2

Table 5 Activation energies for the tested electrodes in kJ/mol

Sample	S1	S2	S3	S4	S5	S6	S7
Energy (KJ mol^{-1})	–	109.1	111.3	85.7	90.5	102.1	100.7

ly decrease this problem. However, the high mobility of calcium might be a problem [22]. This issue will be further addressed in the near future.

The electrochemical performance of the GSFC/CGO10 composite electrode is superior to the performance of most other SOFC cathodes[2]. There may be numerous reasons for this. One could be that the surface segregation of A-site cations is less for the Gd compound than for the La compound. This will result in a surface with more of the catalytic active elements Fe and Co. Another reason could be the creation of a two-phase structure with unique electrocatalytic properties. This is not revealed by the SEM micrographs for the symmetrical cells, but has been observed for dense cells [23]. However, it is noteworthy that a difference in performance of over 100 times between $(La_{0.6}Sr_{0.4})_{0.99}Fe_{0.8}Co_{0.2}O_{3-\delta}$ and GSFC when measured on cone-shaped electrodes only gives a factor of improvement of approximately 2–3 when the performance of the porous composite electrodes is investigated [11, 24]. This can be due to several reasons. One issue is that the microstructure is not the same. In this case, the microstructure is not optimised, and it might be further optimised. It is, however, doubtful that this is the only reason. Another possible explanation could be that other processes dominate when working with porous electrodes. One of these processes could be surface diffusion of oxygen. This is related to the microstructure of the composite cathodes. Another reason could be that the oxygen ionic conductivity perhaps is lower than for the corresponding La compound due to larger tension in the perovskite lattice [25]. The electronic conductivity is also lower for the Gd compound than for the corresponding La compound [24]. This might give problems with the in-plane conductivity of the composite electrodes.

The EIS measurements are as typically seen for composite cathodes see, i.e. [26]. It has been tried to deconvolute the spectra by comparing with the article by Juhl Jørgensen and Mogensen concerning LSM/YSZ composite cathodes [27]. The low-frequency arc obtained at the highest measured temperature is probably related to diffusion of oxygen in a stagnant gas layer above the electrode, as n has the value 1. At lower temperature, it is not possible to distinguish this arc from the other arcs present in the spectres. As this arc is temperature-independent, this is as expected. No knowledge concerning the high-frequency arc obtained at 600 °C is known. The high-frequency arc at the highest measured temperatures equals the low-frequency arc at the lowest measured temperatures, as evaluated on background on the activation energy plot, see Fig. 7. This arc seems to be arc C in the

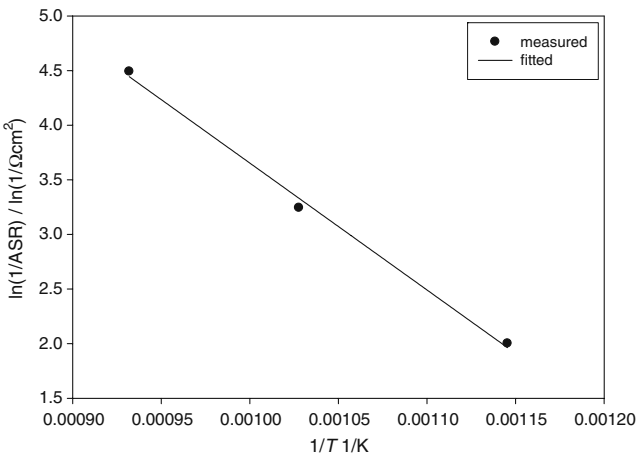

Fig. 7 Activation energy plot of the intermediate arc for sample S7

[2] In general, the ASR values are in the range 0.12 to 0.18 Ωcm^2 at 600 °C.

article by Juhl Jørgensen and Mogensen [27] as it fit with summit frequency as a function of sintering temperature (increases with decreasing sintering temperature), the magnitude of the summit frequencies is also within the range given in the article by Juhl Jørgensen and Mogensen [27] and the activation energy (1.51 eV) is also the same. This arc is related to dissociative adsorption, transfer of species at the TPB and surface diffusion. This arc is always present for LSM/YSZ cathodes. Therefore, it seems that different rate-limiting processes are present at high and low temperatures. The activation energy plot of the total ASR values reveals that the activation energy is lower for the cells sintered at the highest temperatures investigated in this study, see Table 4. This shows that the performance of the cathodes in the relatively low-temperature region is more sensitive to the sintering temperature of the cathodes than the performance of the cathodes at high temperature. This could be due to a better particle–particle contact obtained when the cathodes are sintered at higher temperatures. The dependence of the composition of the cathodes is also displayed in a difference in activation energy being highest for compositions with a low content of CGO10. Whereas the performance at high temperature is almost independent of composition, a large difference is found at the relative low temperatures. This indicates that the performance of the cathodes at low temperature is determined by the ionic conductivity of the cathodes. At low temperature (400 °C or below), an additional arc is revealed. This arc is also observed for LSM/YSZ cathodes at low temperature [28] and can possibly be related to the electrolyte. However, to fully understand the electrochemistry of these composite cathodes, a more in-depth investigation is needed. That the cathodes with a higher content of CGO10 reveal a better performance than the electrodes with a lower content of CGO10 might be due to the formation of a percolation pathway for the oxide anions when the CGO10 content exceeds 30% (*w*/*w*). The GSFC perovskite might be more sensitive to this than the corresponding La compound if the oxide ionic conductivity is lower. The percolation of the CGO10 phase will extend the triple-phase boundary and thereby increase the performance of the cathodes.

Conclusion

High-performance composite cathodes consisting of a mixture between GSFC and CGO10 have been developed. The best composite cathode revealed an ASR as low as 0.12 Ωcm^2 at 600 °C. The composite cathode cannot be used on zirconia-based electrolytes but were compatible with ceria-based electrolytes. The reaction with zirconia was severe at a process temperature of 1,000 °C and it was still too high even at a process temperature as low as 900 °C.

Acknowledgements Colleagues at the Fuel Cells and Solid State Chemistry Division are thanked for fruitful discussions and encouragement. The Danish Energy Agency is thanked for financial support (j. nr. 33030-0109).

References

1. Minh NQ, Takahashi T (1995) Science and technology of ceramic fuel Cells. Elsevier
2. Lee HY, Jang JH, Oh SM (1999) J Electrochem Soc 146:1707
3. Yamamoto O, Takeda Y, Kanno R, Noda N (1987) Solid State Ionics 22:241
4. Brugnoni C, Ducati U, Chemelli C, Scagliotti M, Chiodelli G (1995) Solid State Ionics 76:183–188
5. Takeda Y, Yamamoto O, Kanno R, Noda N, Tomida Y (1987) J Electrochem Soc 134:2656
6. Ullmann H, Trofimenko N, Tietz F, Stover D, Ahmad-Khanlou A (2000) Solid State Ionics 138:79
7. Xia CR, Rauch W, Chen FL, Liu ML (2002) Solid State Ionics 149:11
8. Sahibzada M, Steele BCH, Zheng K, Rudkin RA, Bae JM, Kiratzis N, Metcalfe IS (1996) Proc. 2nd European Solid Oxide Fuel Cell Forum, Oslo, p 687
9. Sahibzada M, Benson SJ, Rudkin RA, Kilner JA (1998) Solid State Ionics 115:285
10. Murray EP, Sever MJ, Barnett SA (2002) Solid State Ionics 148:27
11. Wang WG, Mogensen M (2005) Solid State Ionics 176:457
12. Shao Z, Haile SM (2004) Nature 431:170
13. Ralph JM, Schoeler AC, Krumpelt M (2001) J Mat Science 36:1161
14. Chick LA, Pederson LR, Maupin GD, Bates JL, Thomas LE, Exarhos GJ (1990) Materials Letters 10:6
15. Boukamp BA (1989) Equivalent circuit. University of Twente
16. Jacobsen T, Zachau-Christiansen B, Bay L, Skaarup S (1996) in High temperature electrochemistry: ceramics and metals. Poulsen FW, Bonanos N, Linderoth S, Mogensen M, Zachau-Christiansen B, Editors, 17th Risø International Symposium on Materials Science, Roskilde, DK. p 29
17. Dyck CR, Peterson RC, Yu ZB, Krstic VD (2005) Solid State Ionics 176:103
18. Riza F, Ftikos C, Tietz F, Fischer W (2002) J European Ceramic Soc 22:591
19. JCPDS 15-0196
20. Shannon RD (1976) Acta Cryst A32:751
21. Wang WG, Barfod R, Larsen PH, Kammer K, Bentsen JJ, Hendriksen PV, Mogensen M (2003) *Electrochem Soc Proc* 2003-07 400
22. Carter JD, Appel CC, Mogensen M (1996) J Solid State Chem 122:407
23. Kammer K, Søgaard M, Mogensen M (2007) Electrochem Solid-State Lett 10:B119
24. Kammer K (2006) Solid State Ionics 177:1047
25. Mogensen M, Lybye D, Bonanos N, Hendriksen PV, Poulsen FW (2001) Electrochem Soc Proc 2001–28:15
26. Juhl M, Primdahl S, Manon C, Mogensen M (1996) J Power Sources 61:173
27. Jørgensen MJ, Mogensen M (2001) J Electrochem Soc 148:A433
28. Bonanos N, Holtappels P, Jørgensen MJ (2002) Proc. 5th European Solid Oxide Fuel Cell Forum, Lucern, CH. 578